

First Principles Investigation of Magnetic Properties of Fe-Ni-Mn-Al Heusler Alloys

Mikhail A. Zagrebin^{1,2}, Vladimir V. Sokolovskiy¹, Vasilii D. Buchelnikov¹, and Marina A. Klyuchnikova¹

¹ Chelyabinsk State University, Chelyabinsk, Russia

² National Research Sout Ural State University, Chelyabinsk, Russia
miczag@mail.ru

Abstract

The composition dependences of crystal lattice parameters, magnetic moments and magnetic exchange parameters in $\text{Fe}_x\text{Ni}_{2-x}\text{Mn}_{1+y}\text{Al}_{1-y}$ ($0.0 \leq x \leq 2.0$; $0.0 \leq y \leq 0.6$) Heusler alloys are investigated with the help of first principles calculations. Our simulations have shown that crystal lattice parameter is decreased with Fe content (x) increasing. Our calculations show that increase of Fe content (x) leads increasing of magnetic exchange interactions between Mn atoms at regular positions and Mn atoms at Al positions and change of interaction sign from antiferromagnetic type to ferromagnetic one for Fe content $x \geq 1.4$. Competitive behavior between ferromagnetic and antiferromagnetic interactions shows that these alloys have a complex magnetic structure. Calculated data for crystal lattice parameter, magnetic moment and magnetic exchange parameters for pure compounds ($x = 0.0$ and $x = 2.0$) are in an agreement with theoretical and experimental data.

Keywords: Heusler alloys, magnetic exchange interactions, first principles calculations, density functional theory

1 Introduction

Heusler alloys have attracted interest because of number of interesting effects (such as shape memory, magnetocaloric effects, exchange bias and superelasticity) and their potential applications as intelligent functional materials [8, 13, 23]. In recent years, novel $\text{Fe}_{2+x}\text{Mn}_{1-x}\text{Al}$ Heusler compounds have been intensively investigated by experimentalists and theoreticians [2, 18, 6, 10, 27, 4]. These interesting magnetic materials are considered to be very promising for technological applications utilizing their properties such as anomalous behaviours of optical, magnetic and transport properties. Especially interesting behaviour of these compounds is related to the competing ferromagnetic (FM) – antiferromagnetic (AF) exchange interactions between Fe atoms at the order-disorder structural transition from $A2$ to $B2$ structure [18, 6]. Buchelnikov et al. [10] shows that in Fe_2MnAl the ground state of cubic phase is AF, while a

metastable ferrimagnetic (FIM) state is also present, being higher in energy only by an order of kT , suggesting a close competition of these two magnetic states in real materials. The FIM state corresponds better to the experimental data. Among the Ni-Mn-based FSMA, Ni-Mn-Al system has received much less attention up to now. Stoichiometric Ni_2MnAl is structurally stable down to the lowest temperatures, but martensitic transformations occur in the slightly off-stoichiometric compounds, and their mechanical properties are more favorable than those of the relatively brittle Ni_2MnGa [14, 1]. Experiments show that in off-stoichiometric alloys a competition mechanism between ferromagnetism and antiferromagnetism should be expected [21]. Fe-Ni-Mn-Al alloys have attracted interest recently [16, 5, 19, 20, 24, 26, 7]. In [19, 20, 24] the super-elastic behavior was observed over a temperature range from 77 to 513 K for composition $\text{Fe}_{43.5}\text{Ni}_{7.5}\text{Mn}_{34}\text{Al}_{15}$. $\text{Fe}_{30}\text{Ni}_{20}\text{Mn}_{35}\text{Al}_{15}$ alloy demonstrates good room-temperature strength and significant ductility [16, 5]. Investigations show that in $\text{Ni}_{44}\text{Fe}_6\text{Mn}_{32}\text{Al}_{18}$ positive value of magnetic entropy change was 3.35 J/kg K in the field change of 30 kOe [26]. All these results suggest that $\text{Fe}_x\text{Ni}_{2-x}\text{Mn}_{1+y}\text{Al}_{1-y}$ alloys would be the promising candidates for magnetic multifunctional materials.

In view of the aforesaid, in this work, we will present the *ab initio* calculations of magnetic properties of $\text{Fe}_x\text{Ni}_{2-x}\text{Mn}_{1+y}\text{Al}_{1-y}$ ($0.0 \leq x \leq 2.0$; $0.0 \leq y \leq 0.6$) compounds.

2 Calculation details

All calculations were performed using the density functional theory as part of the spin-polarized relativistic Korringa-Kohn-Rostoker (SPR-KKR) package [11, 12]. This code is based on the KKR-Greens function formalism that uses the multiple-scattering theory, and the electronic structure is expressed in terms of the corresponding Greens function as opposed to Bloch wave functions and eigenvalues. In this code, chemical disorder is treated through the coherent potential approximation (CPA) [12]. The SPR-KKR was used to determine the optimized lattice parameters with $L2_1$ unit cell which consist of the 4-atoms for ferromagnetic state in which all magnetic moments of Fe, Ni and Mn atoms are parallel (Al atom has small magnetic moment and it has not been taken into account) [10, 27]. For the optimized lattice parameter the Heisenbergs magnetic exchange coupling parameters J_{ij} were calculated. The exchange coupling parameters J_{ij} within a real-space approach were calculated using an expression proposed by Liechtenstein et al. [17]. In our calculations we used the generalized gradient approximation for the exchange correlation functional in the formulation of Perdew, Burke and Ernzerhof (PBE) [22].

We used $L2_1$ structural phase with space group of $Fm\bar{3}m$ (225), which consists of four interpenetrating face-centred cubic sublattices. In this structure Al atoms occupy the sites (0; 0; 0); Mn occupy (1/2; 1/2; 1/2) ones; Fe and Ni atoms are randomly located at the sites (1/4; 1/4; 1/4) and (3/4; 3/4; 3/4). The location of addition Mn atoms was assumed to be at Al-site [10, 27, 3]. It should be noted that we will use following designations such as Mn_1 and Mn_2 . Here, Mn atoms, which are located at regular Mn sublattice, are denoted as Mn_1 , whereas Mn_2 designation corresponds to Mn atoms which occupied the Al sublattice.

3 Results of the first principles calculations

3.1 Lattice relaxation

Values of equilibrium lattice constants which have been used in our calculations are listed in Table 1.

	Equilibrium lattice constants a , Å			
	$y = 0.0$	$y = 0.2$	$y = 0.4$	$y = 0.6$
$x = 0.0$	5.843	5.852	5.864	5.874
	5.822 ^a			
$x = 0.2$	5.832	5.834	5.838	5.879
$x = 0.6$	5.814	5.820	5.829	5.836
$x = 1.0$	5.813	5.813	5.815	5.811
$x = 1.4$	5.804	5.794	5.784	5.772
$x = 1.8$	5.793	5.778	5.757	5.736
$x = 2.0$	5.797	5.772	5.746	5.722
	5.787 ^b			

Table 1: Calculated equilibrium lattice constants a of $\text{Fe}_x\text{Ni}_{2-x}\text{Mn}_{1+y}\text{Al}_{1-y}$ in austenite state. ^a Reference [25], ^b Reference [10].

As you can see equilibrium lattice constants decrease in general with increasing of Fe excess. These results are in good agreement with lattice constants for Ni_2MnAl and Fe_2MnAl obtained from experiment [25] and *ab initio* calculations for FM state [10]. Obtained values of lattice constant are used for further calculations of magnetic properties of $\text{Fe}_x\text{Ni}_{2-x}\text{Mn}_{1+y}\text{Al}_{1-y}$ alloys.

3.2 Magnetic moment

The calculations of partial and total magnetic moments of $\text{Fe}_x\text{Ni}_{2-x}\text{Mn}_{1+y}\text{Al}_{1-y}$ alloys have been done by means of the SPR-KKR package. In Fig. 1a we present the composition dependencies of the total magnetic moment, whereas partial moments for each sort of atoms as function of Fe excess x are depicted in Fig. 1b- 1f.

As you can see from Fig. 1a for low content of Fe difference between values of total magnetic moments is approximately equal to $0.9\mu_B$ and equal to $\approx 4\mu_B$, $\approx 5\mu_B$, $\approx 6\mu_B$ and $\approx 7\mu_B$ for $y = 0.0$, $y = 0.2$, $y = 0.4$ and $y = 0.6$ respectively. For high content of Fe it is approximately $\mu_B/4$. For $y = 0.0$ and $y = 0.2$ magnetic moment increases (approximately to $0.8\mu_B$) with increasing of Fe excess while for $y = 0.4$ and $y = 0.6$ magnetic moment increases until $x = 1.0$ and then decreases. Obtained results are in a good agreement with data from *ab initio* calculations for Fe_2MnAl , $\text{Fe}_{1.0}\text{Ni}_{1.0}\text{MnAl}$, $\text{Fe}_{1.75}\text{Ni}_{0.25}\text{Mn}_{1.25}\text{Al}_{0.75}$ and Ni_2MnAl compositions [7, 9, 10, 3]. Obtained magnetic moment for Ni_2MnAl composition is also in a good agreement with experimental data [25].

Concentration dependence of partial magnetic moment of Fe has complex behavior (Fig. 1b). For low content of Mn ($y = 0.0; 0.2; 0.4$) magnetic moment decreases until $x = 0.6$ and then increases. Fe magnetic moment for $\text{Fe}_x\text{Ni}_{2-x}\text{Mn}_{1.6}\text{Al}_{0.4}$ increases until $x = 0.6$, then decreases until $x = 1.4$ and increases again. Values of partial magnetic moments are approximately equal $1.5\mu_B$.

Partial magnetic moment of Ni increases with increasing of Fe and Mn content. Value of magnetic moment is approximately equal to $0.5\mu_B$. Partial magnetic moment of Mn_1 linearly decreases with increasing of Fe content from $3.5\mu_B$ to $2\mu_B$. The same behavior is observed for partial magnetic moment of Mn_2 atom. Value of Mn_2 for low Fe content is a bit more than Mn_1 . However with increasing of Fe the difference between Mn_1 and Mn_2 magnetic moments decreases and for $x = 2.0$ magnetic moments have the same values. Partial magnetic moment of Al is negative and has values not more than $-0.2\mu_B$. Values of partial magnetic moments for Ni_2MnAl and Fe_2MnAl are the same as in [9, 3].

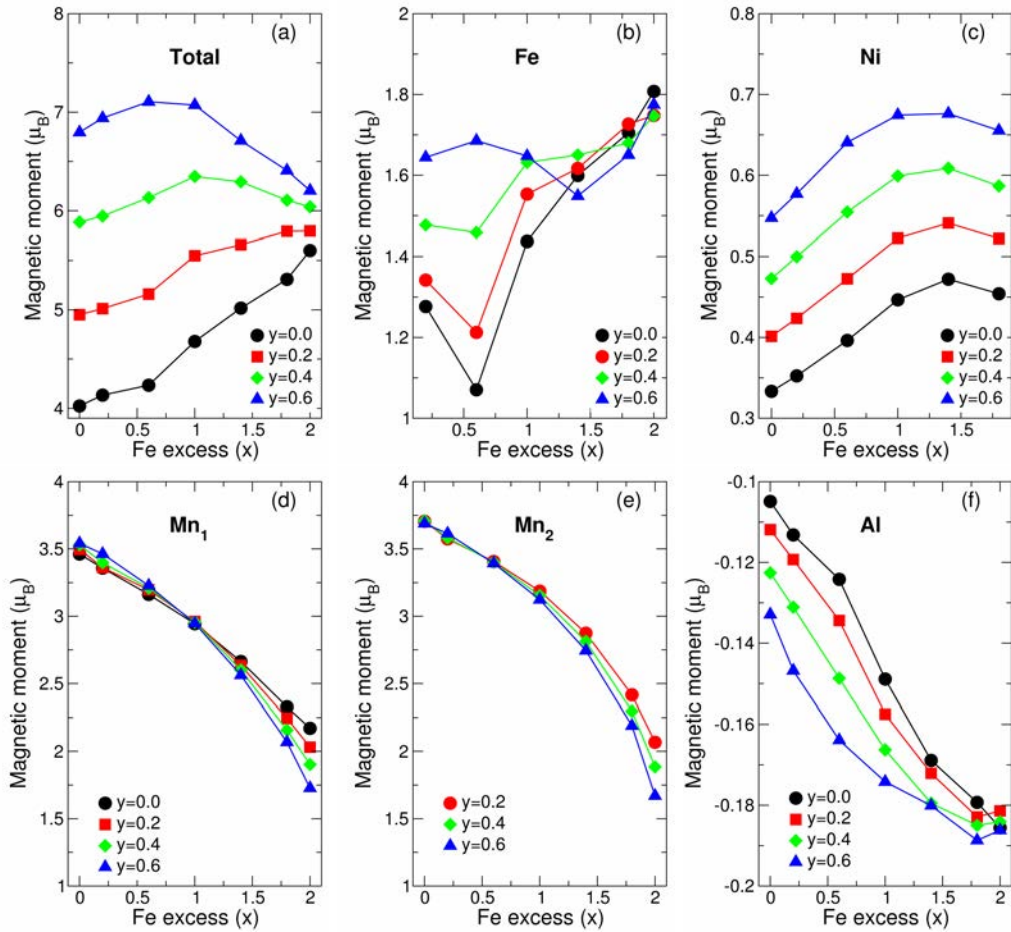


Figure 1: Calculated spin magnetic moment of $Fe_xNi_{2-x}Mn_{1+y}Al_{1-y}$ in austenite phase for different value of Mn excess (y) as a function of Fe excess (x). a) total magnetic moment; b) partial magnetic moment of Fe atoms; c) partial magnetic moment of Ni atoms; d) partial magnetic moment of Mn₁ atoms; e) partial magnetic moment of Mn₂ atoms; f) partial magnetic moment of Al atoms.

3.3 Magnetic exchange parameters

Fig. 2 displays the magnetic exchange parameters for $Fe_xNi_{2-x}Mn_{1+y}Al_{1-y}$ in austenite phase as a function of a distance between pairs of atoms. Here and further, the positive exchange constants ($J_{ij} > 0$) are presented a FM coupling, whereas the negative ones ($J_{ij} < 0$) indicate an AF coupling. The oscillating damped behavior of J_{ij} can be observed. We would like to note that this trend is typical for RKKY-exchange [15]. In the case of austenitic phase of $Fe_{0.2}Ni_{1.8}Mn_{1.0}Al_{1.0}$ (Fig. 2a) the strongest FM interaction can be found between nearest-neighbor (NN) Fe-Mn₁ and Mn₁-Ni atoms. Note, that value of these interaction is equal approximately to 7 meV. AF interaction can be found between NN Fe-Fe atoms in the first and second coordination sphere. Interaction in third coordination sphere splits on weak FM and strong AF (≈ 6 meV) ones. Fourth NN interaction for Fe-Fe becomes FM. It clearly indicates

on the competition behavior between the FM and AF interactions.

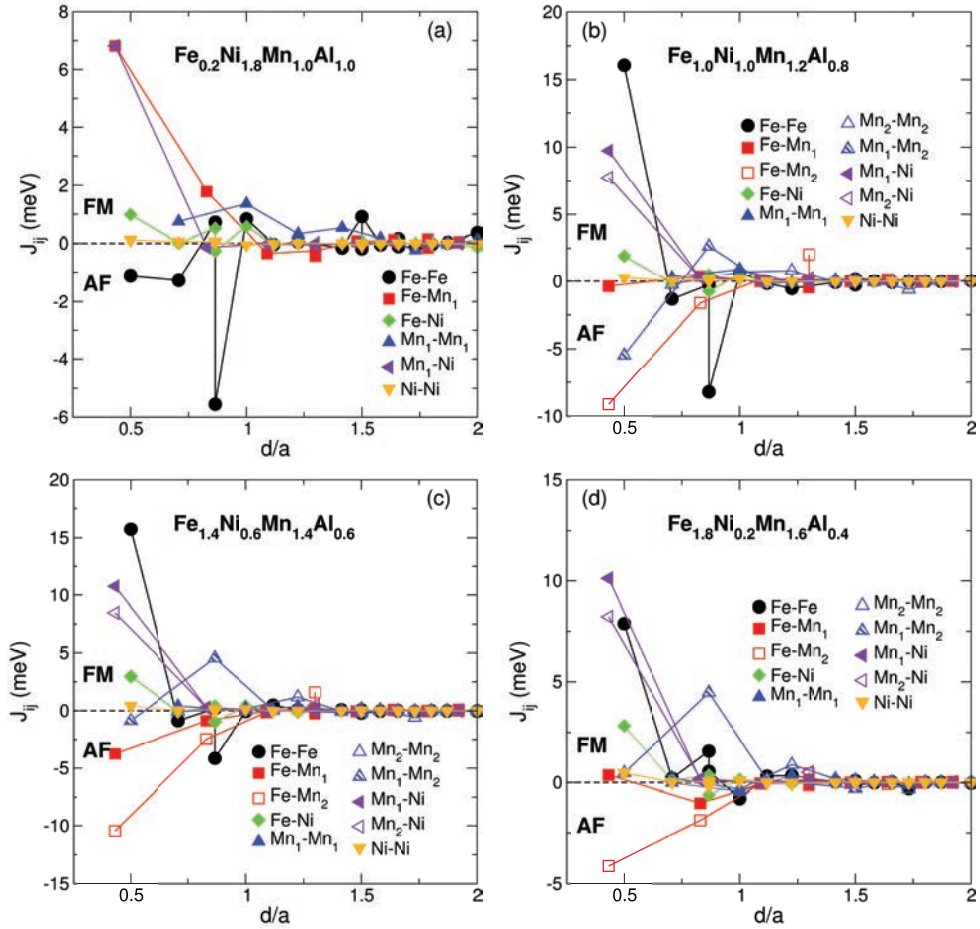


Figure 2: Calculated exchange couplings parameters for $\text{Fe}_x\text{Ni}_{2-x}\text{Mn}_{1+y}\text{Al}_{1-y}$ in austenite phase as a function of a distance between pairs of atoms i and j (in units of the lattice constant a). a) $\text{Fe}_{0.2}\text{Ni}_{1.8}\text{Mn}_{1.0}\text{Al}_{1.0}$; b) $\text{Fe}_{1.0}\text{Ni}_{1.0}\text{Mn}_{1.2}\text{Al}_{0.8}$; c) $\text{Fe}_{1.4}\text{Ni}_{0.6}\text{Mn}_{1.4}\text{Al}_{0.6}$; d) $\text{Fe}_{1.8}\text{Ni}_{0.2}\text{Mn}_{1.6}\text{Al}_{0.4}$.

For $\text{Fe}_{1.0}\text{Ni}_{1.0}\text{Mn}_{0.8}\text{Al}_{1.2}$ (Fig. 2b) first NN interaction for Fe-Fe becomes strongly FM ($J_{\text{Fe-Fe}} \approx 16$ meV), while in other coordination spheres behavior is the same. First Fe- Mn_1 interaction decreases until to weak AF while first Mn_1 -Ni interaction increases up to 10 meV. Interaction between first NN Mn_2 -Ni is FM ($J_{\text{Mn}_2\text{-Ni}} \approx 7.5$ meV) and interactions between Fe- Mn_2 and Mn_1 - Mn_2 are AF ($J_{\text{Fe-Mn}_2} \approx -5$ meV and $J_{\text{Mn}_1\text{-Mn}_2} \approx -10$ meV).

For $\text{Fe}_{1.4}\text{Ni}_{0.6}\text{Mn}_{1.4}\text{Al}_{0.6}$ (Fig. 2c) this behavior remains unchanged except Mn_1 - Mn_2 interaction. For this composition Mn_1 - Mn_2 interaction decreases.

For composition $\text{Fe}_{1.8}\text{Ni}_{0.2}\text{Mn}_{1.6}\text{Al}_{0.4}$ interaction between Fe-Fe in third coordination sphere splits on two FM interactions in comparison with previous dependence (see Fig. 2d).

Magnetic exchange parameters in the first coordination sphere in austenite state of $\text{Fe}_x\text{Ni}_{2-x}\text{Mn}_{1+y}\text{Al}_{1-y}$ as a function Fe content (x) are depicted in Fig. 3. From Fig. 2 you

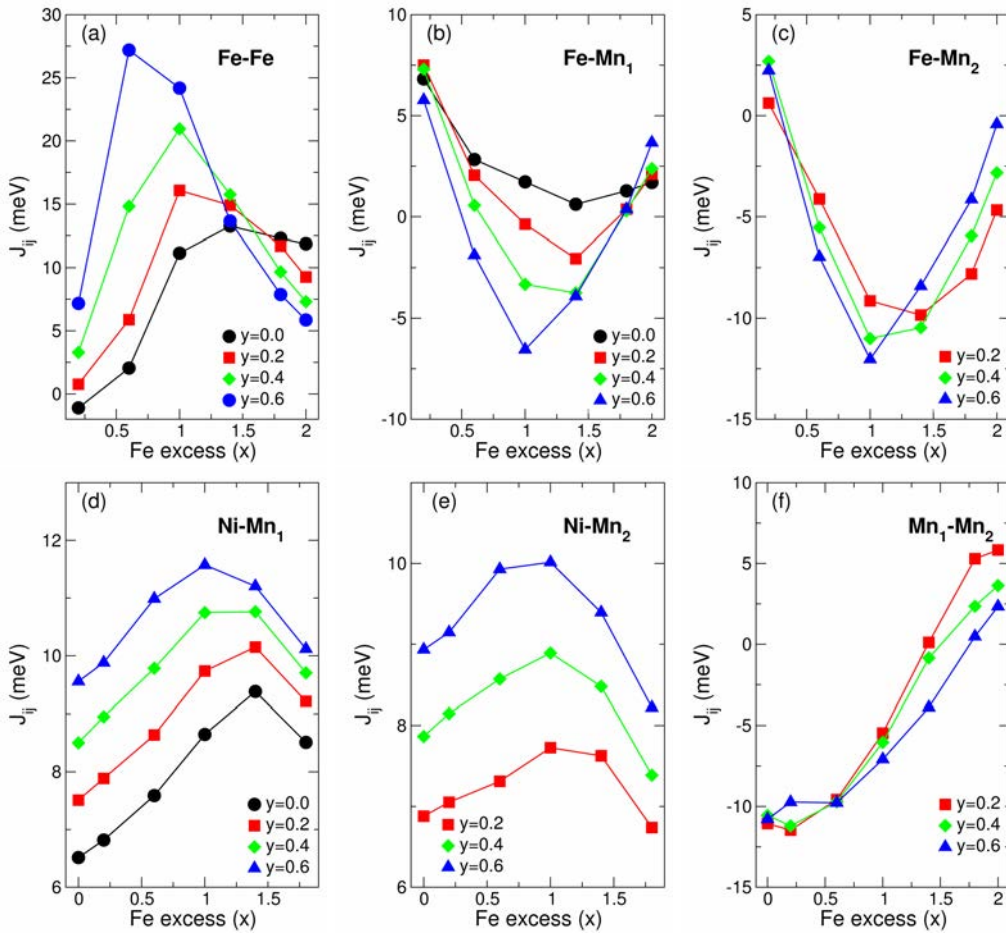


Figure 3: The magnetic exchange parameters J_{ij} in the first coordination sphere for $\text{Fe}_x\text{Ni}_{2-x}\text{Mn}_{1+y}\text{Al}_{1-y}$ in austenite phase as a function of Fe excess (x). a) Fe-Fe coupling; b) Fe-Mn₁ coupling; c) Fe-Mn₂ coupling; d) Ni-Mn₁ coupling; e) Ni-Mn₂ coupling; f) Mn₁-Mn₂ coupling.

can see that interactions between Ni-Ni, Fe-Ni, Mn₁-Mn₁, Mn₂-Mn₂ atoms are weak and not shown on the Fig. 3.

It can be observed from Fig. 3 that the substitution of Ni with Fe leads to an increase in the first NN Mn₁-Mn₂ interactions as compared to $\text{Fe}_{0.2}\text{Ni}_{1.8}\text{Mn}_{1.0}\text{Al}_{1.0}$ alloy from AF ($J_{AF} \approx -12$ meV) to FM ($J_{FM} \approx 5$ meV). Interactions between Ni-Mn_{1,2} increases until $x = 1.4$ (for $y = 0.0$) and $x = 1.0$ (for the remaining y concentration) and then decreases. For $x = 1.4$ maximum is approximately 9 meV and for $x = 1.0$ maximum is approximately 11 meV. For Fe-Mn_{1,2} behavior is opposite: interaction decreases until $x = 1.4$ increase (for $y = 0.0$) and $x = 1.0$ (for the remaining y concentration) and then increases. Note, that interactions after $x \approx 0.5$ becomes AF ($J_{AF} \approx 8-12$ meV). Interaction between Fe-Mn₂ for $\text{Fe}_{1.8}\text{Ni}_{0.2}\text{Mn}_{1.6}\text{Al}_{0.4}$ increases up to weak FM. Note, that AF interaction between Fe-Mn₂ stronger than interaction between Fe-Mn₁. Behavior of interaction between Fe-Fe NN is more complicated. For $y = 0.0$ this

interaction increases with increasing of Fe concentration. For $y = 0.2$ and $y = 0.4$ interaction increases until 15 and 20 meV (respectively) at $x = 1.0$ and then decreases. For $y = 0.6$ maximum reached at $x = 0.6$ and is approximately 27 meV. Obtained results for interactions between Fe-Fe and Fe-Mn₁ for Fe₂MnAl are in a good agreement with data from *ab initio* calculations [27].

4 Summary

The composition dependence of crystal lattice parameters, magnetic moments and magnetic exchange parameters in Fe_xNi_{2-x}Mn_{1+y}Al_{1-y} ($0.0 \leq x \leq 2.0$; $0.0 \leq y \leq 0.6$) Heusler alloys are investigated with the help of first principles using the SPR-KKR method. Crystal lattice parameter is decreased with Fe content (x) increasing. An increase of Fe content results to increase of magnetic exchange interactions between Mn atoms at regular positions and Mn atoms at Al positions to change of interaction sign from AF type to FM one for Fe content $x \geq 1.4$. Competitive behavior between FM and AF interactions shows that these alloys have a complex magnetic structure. Calculated data for pure compounds ($x = 0.0$ and $x = 2.0$) is in an agreement with theoretical and experimental data. It should be noted that for more complete understanding of crystal and magnetic structure it is necessary to investigate different magnetic structures.

5 Acknowledgments

This work was supported by Russian Science Fund No. 14-12-00570 (Section 1), Ministry of Education and Science RF No. 3.2021.2014/K (Section 2), RFBR (grants 14-02-01085, 14-02-31189).

References

- [1] M. Acet, E. Duman, and E.F. Wassermann. Coexisting ferro- and antiferromagnetism in Ni₂MnAl Heusler alloys. *J. Appl. Phys.*, 92(7):3867–3871, 2002.
- [2] G.A. Perez Alcazar, L.E. Zamora, and A. Bohorquez. Magnetic phase diagram of the Fe_xMn_{0.6-x}Al_{0.40} alloys series. *J. Appl. Phys.*, 79(8):6155, 1996.
- [3] A. Ayuela, J. Enkovaara, K. Ullakko, and R.M. Nieminen. Structural properties of magnetic Heusler alloys. *J. Phys.: Condens. Matter*, 11:2017–2026, 1999.
- [4] S.M. Azar, B.A. Hamad, and J.M. Khalifeh. Structural, electronic and magnetic properties of Fe_{3-x}Mn_xZ (Z = Al, Ge, Sb) Heusler alloys. *J. Magn. Magn. Mater.*, 324(10):1776–1785, 2012.
- [5] I. Baker, X. Wu, F. Meng, and P.R. Munroe. Microstructures and mechanical properties of two-phase FeNiMnAl alloys. *Mater. Sci. Forum*, 783–786:2549–2554, 2014.
- [6] H. Bremers, J. Hesse, H. Ahlers, J. Sievert, and D. Zachmann. Order and magnetic properties of Fe_{89-x}Mn₁₁Al_x alloys: magnetization measurements and x-ray diffraction. *J. Alloys Compd*, 366(1):67–75, 2004.
- [7] V.D. Buchelnikov, M.A. Klyuchnikova, M.A. Zagrebin, and V.V. Sokolovskiy. First principles investigations of structural and magnetic properties of Fe-Ni-Mn-Al Heusler alloys. *Sol. State Phenom.*, 233–234:187–191, 2015.
- [8] V.D. Buchel’nikov, A.N. Vasiliev, V.V. Koledov, S.V. Taskaev, V.V. Khovailo, and V.G. Shavrov. Magnetic shape-memory alloys: phase transitions and functional properties. *Phys. Usp.*, 49(8):871–877, 2006.

- [9] V.D. Buchelnikov, M.A. Zagrebin, V.V. Sokolovskiy, and I.A. Taranenko. Investigations of crystal and magnetic properties of Fe-Mn-Al alloys from first principles calculations. *Bulleten of Chelyabinsk State University – Vestnik Chelyabinskogo gosudarstvennogo universiteta (in russian)*, 316(18):9–18, 2013.
- [10] V.D. Buchelnikov, M.A. Zagrebin, V.V. Sokolovskiy, I.A. Taranenko, and A. T. Zayak. Investigation of structural and magnetic properties of Heusler $\text{Fe}_{2+x}\text{Mn}_{1-x}\text{Al}$ alloys by first principles method. *Phys. Status Solidi C*, 11(5–6):979–983, 2014.
- [11] H. Ebert. SPRKKR package (version 6.3). <http://ebert.cup.uni-muenchen.de/>.
- [12] H. Ebert, D. Kodderitzsch, and J. Minar. Calculating condensed matter properties using the kkr-greens function method recent developments and applications. *Rep. Prog. Phys.*, 74(9):096501–49, 2011.
- [13] P. Entel, M.E. Gruner, A. Dannenberg, M. Siewert, S.K. Nayak, H.C. Herper, and V. Buchelnikov. Fundamental aspects of magnetic shape memory alloys: Insights from ab initio and monte carlo studies. *Mater. Sci. Forum*, 635:3–12, 2010.
- [14] R. Kainuma, F. Gejima, Y. Sutou, I. Ohnuma, and K. Ishida. Ordering, martensitic and ferromagnetic transformations in Ni-Al-Mn Heusler shape memory alloys. *Mater. Trans.*, 41(8):943–949, 2000.
- [15] C. Kittel. *Introduction to Solid State Physics*. Wiley & Sons Inc., 8 edition, 2005.
- [16] Y. Liao and I. Baker. Microstructure and room-temperature mechanical properties of $\text{Fe}_{30}\text{Ni}_{20}\text{Mn}_{35}\text{Al}_{15}$. *Mater. Charact.*, 59(11):1546–1549, 2008.
- [17] A.I. Liechtenstein, M.I. Katsnelson, V.P. Antropov, and V.A. Gubanov. Local spin density functional approach to the theory of exchange interactions in ferromagnetic metals and alloys. *J. Magn. Magn. Mater.*, 67(1):65–74, 1987.
- [18] X.J. Liu, S.M. Hao, L.Y. Xu, Y.F. Guo, and H. Chen. Experimental study of the phase equilibria in the Fe-Mn-Al system. *Metall. Mater. Trans. A*, 27(9):2429–2435, 1996.
- [19] T. Omori, K. Ando, M. Okano, X. Xu, Y. Tanaka, I. Ohnuma, R. Kainuma, and K. Ishida. Superelastic effect in polycrystalline ferrous alloys. *Science*, 333:68–71, 2011.
- [20] T. Omori, M. Okano, and R. Kainuma. Effect of grain size on superelasticity in Fe-Mn-Al-Ni shape memory alloy wire. *APL Materials*, 1:032103–9, 2013.
- [21] C. Paduani, A. Migliavacca, M.L. Sebben, J.D. Ardisson, M.I. Yoshida, S. Soriano, and M. Kalisz. Ferromagnetism and antiferromagnetism in $\text{Ni}_{2+x+y}\text{Mn}_{1-x}\text{Al}_{1-y}$ alloys. *Solid State Commun.*, 141(3):145–149, 2007.
- [22] J.P. Perdew, K. Burke, and M. Ernzerhof. Generalized gradient approximation made simple. *Phys. Rev. Lett.*, 77(11):3865, 1997.
- [23] V. Sokolovskiy, M. Zagrebin, and V. Buchelnikov. Novel achievements in the research field of multifunctional shape memory Ni-Mn-In and Ni-Mn-In-Z Heusler alloys. *Mater. Sci. Foundations*, 81–82:38–76, 2015.
- [24] L.W. Tseng, Ji. Ma, S.J. Wang, I. Karaman, M. Kaya, Z.P. Luod, and Y.I. Chumlyakov. Superelastic response of a single crystalline FeMnAlNi shape memory alloy under tension and compression. *Acta Mater.*, 89:374–383, 2015.
- [25] P.J. Webster, K.R.A. Ziebeck, S.L. Town, and M.S. Peak. Magnetic order and phase transformation in Ni_2MnGa . *Philpos. Mag.*, 49(3):295–310, 1984.
- [26] H.C. Xuan, Y.Q. Zhang, H. Li, P.D. Han, D.H. Wang, and Y. W. Du. The martensitic transformation and magnetic properties in $\text{Ni}_{50-x}\text{Fe}_x\text{Mn}_{32}\text{Al}_{18}$ ferromagnetic shape memory alloys. *Appl. Phys. A.-Mater.*, 119(2):597–602, 2015.
- [27] M.A. Zagrebin, V.D. Buchelnikov, V.V. Sokolovskiy, I.A. Taranenko, and S.I. Saunina. First principles calculations of magnetic exchange parameters of Fe-Mn-Al Heusler alloys. *Sol. State Phenom.*, 215:131–136, 2014.